CPUH-Research Journal: **2016**, ***1(1)***, 47-51
ISSN (Online): 2455-6076
http://www.cpuh.in/academics/academic_journals.php

Effect of Cobalt Doping on Physical Properties of ZnO Nanoparticles

Neha Sharma[1], Shaveta Thakur[1], Ruchita Sharma[1] and Jitender Kumar[2*]

[1]*Department of Physics, Arni University, Kangra (Himachal Pradesh)*

[2] *Department of Physics, Career Point University, Hamirpur (HP) INDIA*

E-mail: *jiten.arni@gmail.com*

(Received 25 Aug, 2015; Accepted 03 Sept, 2015; Published 03 Mar, 2016)

ABSTRACT: Nanocrystals of undoped and Cobalt doped Zinc Oxide nanoparticles (Zn_{1-x} Co_x O, where x = 0, 0.2 and 0.3M) were synthesized by simple solution route. Crystalline phases, optical absorption and band gap of Cobalt doped ZnO nanoparticles/Thin films were studied by X-ray diffraction and UV visible spectrophotometer. XRD results revealed that the sample product was crystalline with a hexagonal wurtzite phase. The particle size was determined by Scherrer method and W-H analysis. In case of Scherrer method and W-H anaylsis, the particle size of cobalt doped ZnO nanoparticles decreases with increase in concentration of cobalt (0, 0.2 and 0.3M) but the particle size of different concentration (0, 0.2 and 0.3M) of cobalt doped ZnO by using W-H analysis is greater than the particle size determined by using Scherrer method. The W-H analysis was used to study the individual contributions of crystallite size and lattice strain on the peak broadening of Co doped ZnO nanoparticles. Nanocrystalline ZnO thin films were prepared by a spin coating technique. The strongest absorption peak appears at around 250nm, which is blue shifted from the absorption edge of bulk ZnO (365nm). The band gap value of prepared cobalt doped ZnO NPs increases with increase in concentration of cobalt doping. Optical studies indicated that nanoparticles had a good transmittance (≅60%) and the band gap increased from 3.2eV to 3.5eV upon Cobalt doping at temperature 500^{o}C.

Keywords: Nanocrystals; Doping XRD and Zinc Oxide.

INTRODUCTION: Nanostructured materials have received much attention because of their novel properties, which differ from those of bulk materials. Control of dimensions and morphology of materials has aroused the interest of researchers in the design of functional devices due to the optical and electronic properties of nanometer and micrometer sized materials, which determine their applications can be adapted by varying their size and shape [1]. Nanoscience and nanotechnology involve studying and working with matter on an ultra small scale from sub nanometer to several hundred nanometers. These nanosize materials have properties that are often significantly different from their counterparts with "ordinary size" [2]. Nanostructured ZnO materials have received broad attention due to their distinguished performance in electronics, optics and photonics. ZnO has a direct wide band gap (3.4eV) at room temperature, which is n-type semiconductor, used in optoelectronics devices because of its high optical transparency. In some cases, it is preferred to be used in n-type doping [3]. In ambient conditions, ZnO has a stable hexagonal wurtzite structure with lattice spacing a=0.325nm and c= 0.521 nm and composed of a number of alternating planes with tetrahedrally coordinated O^{2-} and Zn^{2+} ions. ZnO is known as an important semiconductor which has been studied extensively in the past few years due to its fundamental and technological importance. This semiconductor has several favorable properties: good transparency, high electron mobility, wide band gap, large exciton binding energy and excellent chemical stability and suggest a great many possible practical applications such as in electronics, field emission devices, gas sensors and varistors [4]. Particle size and optical properties play important role in these applications, which have driven researchers to focus on the synthesis of nanocrystalline ZnO in recent years. Keeping in view the extensive uses of ZnO, various types of synthesis techniques have been formulated over the years. Various chemical methods have been developed to prepare nanoparticles of different materials of interest. Most of the ZnO crystals have been synthesized by vapour deposition method [5], sol-gel method [6] and a thermal method [7]. Solution route is a promising alternative synthetic method because of the low process temperature and easy to control the particle size. In the present work undoped ZnO and Cobalt doped ZnO nanoparticles were synthesized by using simple solution route, which is robust and reliable to control the shape and size of particles without requiring the expensive and complex equipments.

A perfect crystal would extend infinitely in all directions therefore; no crystals are perfect due to their finite size. This deviation from perfect crystallinity leads to a broadening of the diffraction peaks. The two main properties extracted from peak width analysis are the crystallite size and lattice Strain. Crystallite size is a measure of the size of coherently diffracting domains. The crystallite size of the particles is not generally the same as the particle size due to the formation of polycrystalline aggregates [8]. Lattice strain is a measure of distribution of lattice constants arising from crystal imperfections, such as lattice dislocations. Crystallite size and lattice strain affect the Bragg peaks in different ways. Both these effects increase the peak width and intensity and shift the 2θ peak position accordingly. The peak width derived from crystallite size varies as 1/Cosθ, whereas strain varies as tanθ. This difference in behavior as a function of 2θ enables to discriminate between the size and strain effects on peak broadening. The Bragg width contribution from crystallite size is inversely proportional to the crystallite size [9]. In this work, a comparative evaluation of the mean particle size of the undoped and cobalt doped ZnO NPs obtained from powder XRD procedures is reported and the band gap measurements are obtained from optical studies. The strain due to lattice deformation associated with the ZnO NPs heated at 500^{o}C was estimated by Williamson-hall analysis (W-H).

MATERIAL NAD METHODS:

Sample synthesis and geometric characterization: The synthesis of ZnO nanoparticles was carried out by simple solution route. The starting materials, $Zn(CH_3COO)_2.2H_2O$ and $Co(NO_3)_2.6H_2O$ solution were prepared as follows: Solution-A: 1M $Zn(CH_3COO).2H_2O$ was dissolved in the solution containing 80 ml distilled water and 20 ml ethanol and Solution-B: Different concentrations of Co $(NO_3)_2.6H_2O$ was mixed with 80 ml of deionized water and 20ml of ethanol. Mixing these solutions has resulted into solution C. The experiment was performed at room temperature. Then ammonia solution was added into the solution drop by drop. The initial solution contains milky colored precipitates of Zinc acetate at low concentration of ammonia. Separately, a buffer solution was prepared by dissolving appropriate amounts of sodium hydroxide. The buffer solution was then added drop wise to the vigorously stirred solution C until the precipitation occur. Then put the solution at constant temperature for 1 hour. The precipitate was filtered and washed with distilled water. The precipitate was dried at 500°C for 1 hour in muffle furnace. Then grind the dry particles. The cobalt nitrate/ basic zinc acetate dehydrate precipitate was decomposed in cobalt doped zinc oxide.

Preparation of Co doped ZnO thin films using Spin Coater: The deposition of doped zinc oxide by spin coating technique has seen increased research activity over the past several years as the need for high quality zinc oxide thin films has increased. Spin coating is used for the application of thin films and for this were used as substrates. A typical process involves depositing a small puddle of a Fluid resin onto the center of a substrate and then spinning the substrate at high speed (typically around 3000 rpm). After preparing ZnO colloidal solution, thin films were deposited. We used well cleaned glass slides 75 x 25mm square inch slides of thickness 1.35mm as the substrate. Prior to processing, each glass slide was washed sequentially in acetone and distilled water. The glass slides were then dried. This ensures that there is no contamination on the glass surface that could potentially interfere with deposition of ZnO thin films. The substrate is secure properly on to the spin coater, and with the aid of syringe, small amount of colloidal solution carefully dispersed on to the substrate. The spin coater is immediately spun at the rate of 3000rpm for 30 secs.
The crystal structure and the particle size of the thin films were identified using an X-ray diffractometer (XRD Model: D8 Focus). A UV-2501 UV–vis spectrophotometer (SHIMADZU, Japan) with an integrating sphere was used to directly record diffuse reflectance spectra of the pure and Cobalt doped ZnO.

RESULTS AND DISCUSSION:

XRD Analysis: The XRD patterns of the prepared sample are shown in Figure 1. It is clearly seen that the FWHM of the reflection peaks decreases after adding the dopant cations, indicating growth of the crystalline or changes in the crystal strains. There is also a negligible shift in peaks, and their FWHM obviously decreased for the samples that were doped with different concentration of Co compared to the un-doped ZnO-NPs. This shift also corresponds to the strain of the compound and replacement of some Zn cations with Cobalt in each compound. By replacing Co with Zinc in the lattice, the strain changed as shown in the peak shift. Wurtzite lattice parameters such as the values of d, the distance between adjacent planes in the Miller indices (hkl), lattice constants a, b, and c, interplaner angle {the angle ϕ between the planes ($h_1\,k_1\,l_1$), of spacing d_1 and the plane ($h_2\,k_2\,l_2$) of spacing d_2}, and unit cell volumes were calculated from the Lattice Geometry equation presented below [10]. The lattice parameters of the powders heated at

500^0 C with different concentration (0, 0.2 and 0.3M) are summarized in Table1.

$$\frac{1}{d^2} = \frac{4}{3}\left(\frac{h^2 + hk + k^2}{a^2}\right) + \frac{l^2}{c^2} \qquad (1)$$

$$V = \frac{\sqrt{3}\,a^2 c}{2} = 0.866\ a^2 c \qquad (2)$$

$$\text{Cos}\phi = \frac{h_1h_2 + k_1k_2 + \frac{1}{2}(h_1k_2 + h_2k_1) + \frac{3a^2}{4c^2}l_1l_2}{\sqrt{(h_1^2 + k_1^2 + h_1k_1 + \frac{3a^3}{4c^2}l_1^2)(h_2^2 + k_2^2 + h_2k_2 + \frac{3a^2}{4c^2}l_2^2}} \qquad (3)$$

Table 1: The structure parameter of un-doped and Co-doped ZnO NPs heated at 500^0 C

Compound	2theta	hkl	d(Å)	Structure	Lattice parameter(nm)	V(nm^3)	Cos ϕ
Pure ZnO	31.71 34.36	(100) (002)	0.2819 0.2608	Hexagonal	a = 0.325 c/a=1.60	47.65	0
$Co_{0.2}Zn_{0.8}O$	31.73 34.42	(100) (002)	0.2816 0.2602	Hexagonal	a = 0.325 c/a=1.60	47.56	0
$Co_{0.3}Zn_{0.7}O$	31.74 34.43	(100) (002)	0.2817 0.2602	Hexagonal	a = 0.325 c/a=1.60	47.34	0

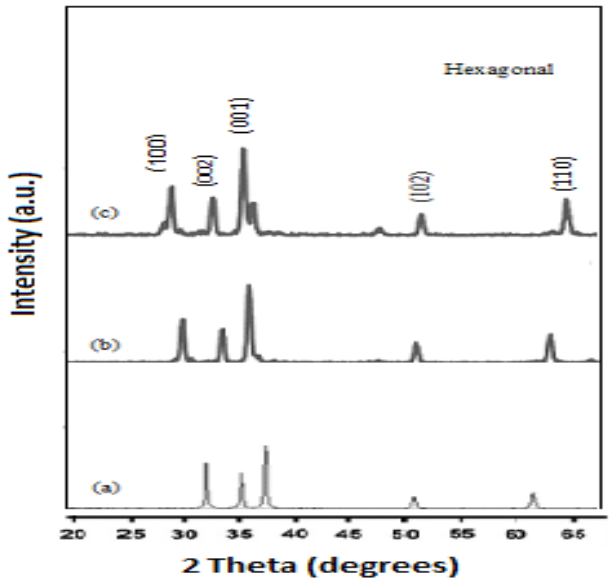

Figure 1: The XRD pattern of Pure ZnO -NPs and Co doped ZnO- NPs heated at 500^0C. (a) Pure ZnO- NPs, (b) Co (0.2M) - doped ZnO- NPs, (c) Co (0.3M) -doped ZnO –NPs; the XRD pattern shows that the samples products are crystalline with a hexagonal Wurtzite phase.

Particle size and strain:

1. Scherrer method: XRD can be utilized to evaluate peak broadening with crystallite size and lattice strain due to dislocation. The crystalline size of the un-doped ZnO and Cobalt doped ZnO with different concentration were determined by the X-ray line broadening method using the Scherrer equation $D = (k\lambda / \beta_D \cos\theta)$, where D is the crystalline size in nanometers, k is a constant equal to 0.94, β_D is the peak width at half maximum intensity, λ is the wavelength of radiation (for CuK_α tion λ =1.54056A^0) and θ is the peak position. Debye Scherrer formula is given as

$$D = \frac{k\lambda}{\beta_D \cos\theta} \qquad (4)$$

$$\text{Cos}\,\theta = \frac{k\lambda}{\beta_D}\left(\frac{1}{D}\right) \qquad (5)$$

2. Williamson-Hall method: The W-H method does not follow a $1/\cos\theta$ dependency as in the Scherrer equation but instead varies with $\tan\theta$. This fundamental difference allows for a separation of reflection broadening when both micro structural causes – small crystallite size and micro strain- occur together. The different approaches presented in the following assume that size and strain broadening are additive components of the total integral breadth of a Bragg peak [11]. Addition of the Scherrer equation and $\epsilon = \beta_s / \tan\theta$ results in following equations:

$$\beta_s = \beta_s + \beta_D \qquad (6)$$

$$\beta_{hkl} = \left(\frac{k\lambda}{D\cos\theta}\right) + (4\epsilon\tan\theta) \qquad (7)$$

Rearranging Eq. (7) gives:

$$\beta_{hkl}\cos\theta = \left(\frac{k\lambda}{D}\right) + (4\epsilon\sin\theta) \qquad (8)$$

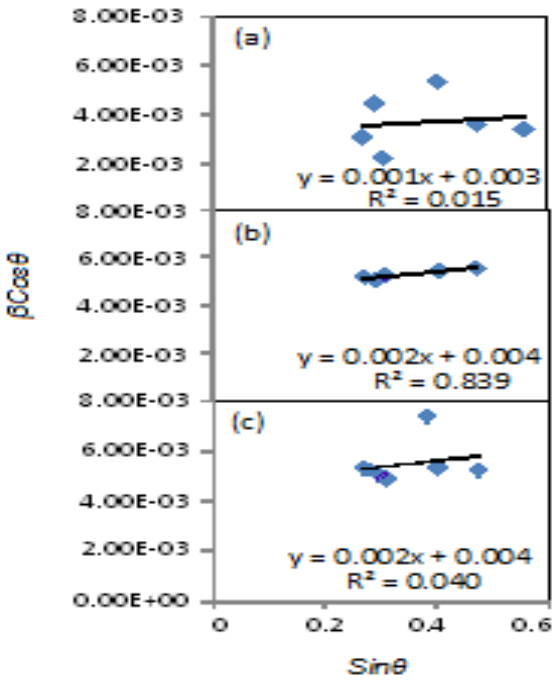

Figure 2: The W-H analysis of Co-doped ZnO NPs heated at 500 ^{0}C (a) Undoped ZnO NPs (b) Co (0.2M) - doped ZnO NPs (c) Co (0.3M) - doped ZnO NPs.

The corresponding Williamson-Hall plot showed that line broadening was essential isotropic (Figure 2). This indicates that the diffracting domains were isotropic and there was also a microstrain contribution. The Particle size of Undoped and Cobalt ZnO nanoparticles was determined by using two methods: Scherrer method and W-H analysis. The W-H analysis was used to study the individual contributions of crystallite size and lattice strain on the peak broadening of Co doped ZnO nanoparticles. From Table 2, it is clear that in case of Scherrer method and W-H anaylsis, the particle size of cobalt doped ZnO nanoparticles decreases with increase in concentration of cobalt but the particle size of different concentration of cobalt doped ZnO by using W-H analysis is greater than the particle size determined by using Scherrer method.

Table 2: Geometric parameters of pure and Co doped ZnO NPs at 500^{o}C

Compound	**Method**	
	Scherrer D(nm)	**W-H Analysis D(nm)**
ZnO	34.22	45.25
$Co_{0.2}Zn_{0.8}O$	27.47	32.168
$Co_{0.3}Zn_{0.7}O$	26.75	30.8

OPTICAL STUDIES: The optical absorption spectra of undoped and cobalt doped ZnO ($Zn_{1-x}Co_xO$, where x= 0, 0.2 and 0.3M) thin films by UV-Vis spectrophotometer in the range 200-800nm were presented. From figure 3, it can be seen that the absorption peak of prepared undoped and cobalt doped thin films appears at 255nm which is fairly blue shifted from the absorption edge of the bulk ZnO. The transmittance quickly decreases below 350 nm due to absorption of light caused by the excitation of electrons from the valence band to conduction band of ZnO. The absorption edge shifted towards longer wavelengths (i.e red shift) with the increase of cobalt doped concentrations. The energy band gap is determined by using the relationship

$$\alpha = A\,(hv - E_g)^n \qquad (10)$$

Where hv = photonic energy, α = absorption coefficient (α = 4πK/λ; k is the absorption index or absorbance, λ is the wavelength in nm), E_g = Energy band gap, A = constant, n = 1/2 for allowed direct band gap. Exponent's n depends upon on the type of transition and it may have values 1/2, 2, 3/2 and 3 corresponding to the allowed direct, allowed indirect, forbidden direct and forbidden indirect transitions respectively

Table 3: Variations of band gap with increase in concentration of Co doped ZnO heated at 500^{0}C.

Compound	***Band gap (eV)***	***Absorption Edge(nm)***
Pure ZnO	*3.50*	*413*
$Co_{0.2}Zn_{0.98}O$	*3.27*	*236*
$Co_{0.3}Zn_{0.97}O$	*3.39*	*224*

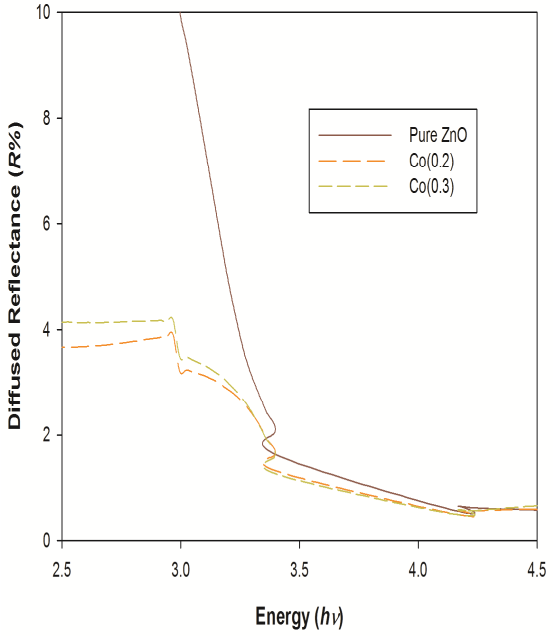

Figure 3: Optical absorption spectra of cobalt doped ZnO nanoparticles with different concentration of Co i.e (a) Undoped ZnO (b) Co(0.2)- doped ZnO- NPs, (d) Co(0.3)-doped ZnO –NPs at 500^{0}C.

From figure 3, it can be seen that excitonic absorption peak of as prepared undoped and with different concentration of cobalt doped Zinc oxide become narrow as the concentration is increases. The sharp exitionic peak in the absorption spectra at 500^{o}C is indicative of the small size distribution of nanocrystal in the samples and broadening of peaks at different concentration clearly indicates the increase in size of nanocrystals with the increase of concentration of Co. It can be observed clearly from table 3 that the absorbance decreases as the concentration increases at 500^{o}C. In Cobalt doped ZnO, an absorption band localized between 200 nm and 350 nm at 500^{o}C. The strongest absorption peak appears at around 250nm, which is blue shifted from the absorption edge of bulk ZnO (365nm). The band gap value of prepared undoped and cobalt doped ZnO NPs increases with increase in concentration of cobalt doping.

CONCLUSION: Nanocrystals of undoped and cobalt doped ZnO NPs ($Zn_{1-x}Co_xO$) were successfully synthesized by using simple solution route. The crystalline structure, optical properties and band gap were determined by XRD and UV-visible spectrophotometer. XRD analysis shows that the prepared samples are in hexagonal wurtzite phase. The particle size can be determined by Scherrer formula, and Williamson Hall analysis. The average size of Co doped ZnO NPs decreases as the concentration of cobalt doping increases. This difference is proportional to strain value and shows that the role of strain is important; therefore, it should be considered in the calculation of crystalline size. Thus, using the Scherrer method without considering strain may yield inaccurate results. Nanocrystalline ZnO thin films were prepared by a spin coating technique. The strongest absorption peak appears at around 250 nm, which is blue shifted from the absorption edge of bulk ZnO (365nm).The band gap value of prepared cobalt doped ZnO NPs increases with increase in concentration of cobalt doping.

ACKNOWLEDGEMENTS: Authors are thankful to Dr. Atul Khanna from Guru Nanak Dev University, Amritsar for technical supports in carrying XRD study.

REFERENCES:

1. Ju-Nam, Y et al. (2008) *Sci Total Environ.* 400(1-3), 396-414.
2. Zhong Lin Wang, (2004) *Journal of Physics: Condensed Matter.* 16 R829- R858.
3. T. Kataoka, Y. Yamazaki, Y. Sakamoto, A. Fujimori, F.-H. Chang, H. J. Lin, et.al. (2010) *Appl. Phys. Lett.* 96, 252502.
4. S. Hingorani, V. Pillai, P. kumar, M. S. Muntai, D. O. Shah, (1993) *Mater. Res. Bull.* 28, 1303.
5. M.R. Vaezi, S.K. Sadrnezhaad, (2007)*Mater. Des.* 28, 515.
6. A. Bandyopadhyay, S. Modak, S. Acharya, A.K. Deb, P.K. Chakarabarti, (2010) *Solid State Sci.*12 , 448.
7. H. Bai, X. Liu, (2010) *Mater. Lett.* 64, 341.
8. K. Ramakanth, Basic of Diffraction and Its Application, I.K. International Publishing House Pvt. Ltd., New Delhi, (2007).
9. V.K. Pecharsky, P.Y. zawali, Fundamentals of Powder Diffraction and Structural Characterization of Materials, Springer, New York, (2003).
10. B. D. Culity, Elements of X-ray Diffraction, Addison-Wesley Publishing Company Inc., California, (1956).
11. M. Birkholz, Thin Film Analysis by X-ray Scattering. Wiley-VCH Verlag GmbH and Co. KGaA, Weinheim (2006).